RC24430 (W0711-159) November 20, 2007
Electrical Engineering

IBM Research Report

An Automated Image Segmentation and Classification Algorithm for Immunohistochemically Stained Tumor Cell Nuclei

Hangu Yeo, Vadim Sheinin
IBM Research Division
Thomas J. Watson Research Center
P.O. Box 218
Yorktown Heights, NY 10598

Yuri Sheinin
Mayo Clinic and Foundation
Rochester, MN 55905

Research Division
Almaden - Austin - Beijing - Cambridge - Haifa - India - T. J. Watson - Tokyo - Zurich

AN AUTOMATED IMAGE SEGMENTATION AND CLASSIFICATION ALGORITHM FOR IMMUNOHISTOCHEMICALLY STAINED TUMOR CELL NUCLEI

Hangu Yeo[1], Vadim Sheinin[1], and Yuri Sheinin[2]

[1]IBM Watson Research Center, Yorktown Heights, NY 10598 USA
[2]Mayo Clinic and Foundation, Rochester, Minnesota 55905 USA

ABSTRACT

As medical image data sets are digitized and the number of data sets is increasing exponentially, there is a need for automated image processing and analysis technique. Most medical imaging methods require human visual inspection and manual measurement which are labor intensive and often produce inconsistent results. In this paper, we propose an automated image segmentation and classification method that identifies tumor cell nuclei in medical images and classifies these nuclei into two categories, stained and unstained tumor cell nuclei. The proposed method segments and labels individual tumor cell nuclei, separates nuclei clusters, and produces stained and unstained tumor cell nuclei counts. The representative fields of view have been chosen by a pathologist from a known diagnosis (clear cell renal cell carcinoma), and the automated results are compared with the hand-counted results by a pathologist.

Keywords: Immunohistochemistry, Medical Image Segmentation and Analysis, and Digital Pathology

1. INTRODUCTION

The quantification of immunohistochemically stained medical image provides numerous technical challenges. More specifically, pathologists quantify immunohistomically stained medical images by manual cell counting, and it is very time consuming process and sometimes produces subjective and inconsistent results. The automated technique capable of replacing traditional pathological examination of the slides from the tumor tissue can produce more objective and stable quantification results than manual cell counting. In the past years, many medical image segmentation and analysis techniques have been presented. Those techniques [1]-[10] are based on morphological techniques, threshold-based techniques, region-based techniques, and so on. Most of these algorithms use initial threshold-based techniques to segment cell nuclei followed by region-based techniques to separate clusters of cell nuclei. Separation of clusters of cell nuclei into individual objects is a very important issue because it may separate clusters into too few objects (under-segmentation) or too many objects (over-segmentation). To improve over-segmentation or under-segmentation of marker-controlled segmentation algorithm, various enhanced marker detection algorithms based on adaptive erosion [4], hierarchical clustering [5], and supervised learning [6]-[8] are introduced, and mathematical morphology based classifiers are proposed in [1]-[3].

In this paper, we have developed an automated image segmentation and classification algorithm which quantifies immunohistochemically stained medical images of a known diagnosis (clear cell renal cell carcinoma). Renal cell carcinoma (RCC) is the most common renal malignancy which represents 3% of adult neoplasms [12]. Clear cell renal cell carcinoma (ccRCC) is a main histological subtype, accounting for more than 80% of RCC [13]. Pathological stage remains the best prognostic factor for RCC. However, new biomarkers are needed to improve prognosis and identify patients with distinct clinical outcome. Survivin is an antiapoptotic protein that belongs to the inhibitor of apoptosis protein family [14]. It has been shown that survivin expression is an independent predictor of ccRCC pregression and death [15]. In tissue, survivin can be reliably detected by means of immunohistochemistry. Automated evaluation of survivin expression might portend valuable information on ccRCC biology. A typical stained image contains many different types of objects such as stained and unstained tumor cell nuclei, stained and unstained lymphocytes, stromal cells, neutrophils, and so on (Figure 1). The proposed algorithm mainly uses pixel intensity information to segment cell nuclei, and color information to identify stained cell nuclei. The threshold-based technique classifies a medical image into a binary image (foreground and background) by grouping all pixels with intensity values greater than a global threshold into one class and other pixels into another class. Segmenting an entire image using only one global threshold value doesn't produce good segmentation result. The robustness of segmentation has been improved by using adaptive segmentation technique based on local threshold values for the foreground object segmentation. The segmented

foreground objects are labeled and basic morphological operations are applied to each object. Simple shape descriptors (area, perimeter, circularity, average intensity value, and so on) are defined and obtained to describe each object. The shape descriptors will be used to identify cell nuclei among foreground objects. The region-based technique is to separate object clusters into separate objects based on region growing and region splitting/merging techniques. We applied a widely used technique called Watershed Transform to separate nuclei clusters into small objects representing individual nucleus. The watershed transform is based on number of markers, and determining correct number of markers is very important to avoid under or over segmentation. The proposed algorithm is based on a modified h-minima transform to overcome under/over segmentation problem. Finally, the cell nuclei are classified into stained or unstained nuclei according to the fraction of stained pixels.

The paper is structured as follows. Section 2 describes our segmentation and classification algorithm with a simple example. Section 3 presents results of the simulation experiments, and conclusions are given in Section 4.

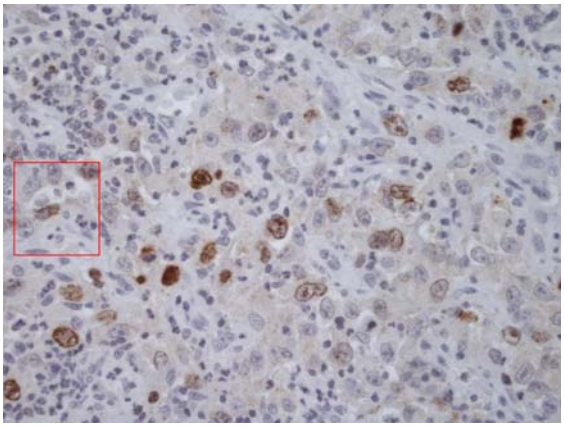

Figure 1: Immunohistochemically stained image.

2. IMAGE SEGMENTATION ALGORITHM

This section briefly describes our proposed image segmentation and classification algorithm. The input images in RGB format are converted into YUV format, and each pixel value is composed of intensity (Y) and color components (U and V). The cell nuclei segmentation is based on pixel intensity and stained and unstained cell nuclei classification is based on the color components. The color conversion is followed by histogram stretching algorithm. The main purpose of the histogram stretching is to improve the contrast considerably by mapping limited input histogram range to the full output histogram range (from 0 to 255).

A simple segmentation technique is applied to the original image to convert it into a binary image with foreground and background objects. We used a segmentation technique proposed by Otsu [10]. Otsu's segmentation method is a widely used thresholding segmentation technique, and the goal is to find a threshold that classifies the entire image into two clusters using pixel intensitie. The segmented binary image is depicted in Figure 2 (b). The Otsu's segmentation method introduces small size objects (salt-and-pepper noise) and holes in large objects. After this initial segmentation process, we label each object, and object shape descriptors are defined and obtained for each object. The background is labeled as 0 and the foreground objects are labeled with integer numbers greater than 0. The descriptors are set of numbers that are produced to describe the shape of a certain object. Simple shape descriptors are defined, and these include area, perimeter, compactness, and circularity. The definitions of shape descriptors are

Area : The number of pixels in an object.
Perimeter : The number of pixels in the boundary of an object.
Compactness : The compactness defines how closely-packed the shape is (compactness = perimeter * perimeter / area).
Circularity : The circularity of a circle is 1, and all other shapes have a circularity less than 1 (circularity = 4π / compactness).

The small size objects such as salt-and-pepper noise is removed based on the descriptor, and holes in large objects are filled by using a simple morphological fill-hole operation. The resulting image is depicted in Figure 2 (c). In some cases the image intensity level varies among different areas through the entire image, and the Otsu's segmentation technique using a single global threshold value introduces missing objects or false objects. To fix this problem, based on the object shape descriptors obtained from the initial segmentation, we segment local regions again to correct the initially segmented image.

The adaptive thresholding segmentation method segments an image into foreground objects and a background, but as noted in Figure 2 (c) the foreground objects include nuclei clusters that need to be separated into small objects representing individual nucleus. The watershed algorithm [11] is a widely used method that segments an image into watershed regions. However, noise and small unimportant fluctuation in the foreground object may cause spurious minima which leads to over-segmentation, and smoothing the image can be an approach to overcome this problem. The algorithm is based on markers and determining the correct number of markers is very important. The markers are obtained by applying distance transform to the segmented objects as the distance transform is very helpful when the segmentation is based on the shape of the objects. Distance transform calculates the

distance for every pixel in each foreground object to the nearest background pixel as shown in Figure 2 (d). The h-minima transform is applied to Figure 2 (d) to extract markers. However, a simple global h-minima transform may produce incorrect number of markers. The h-minima transform is adaptively modified based on the size of a certain object, and this plays a vital role in reducing over segmentation. Now there is one marker obtained for each object, and we apply the watershed transform. The watershed transform defines watershed lines by means of flooding process. It uses the topographical surface with catchment basins obtained from distance transform. When segmenting a dense nucleus cluster, the aforementioned h-minima transform may not work properly, and cannot extract markers for each individual nucleus because the bottleneck connection is not clear as depicted in Figure 2 (c). To enhance this touching nuclei which are too close together to separate, an improved distance transform combining distance transform (Figure 2 (d)) and edge information (Figure 2 (e)) is used. The edge information is extracted using a well-known Sobel edge detection algorithm [12]. The Sobel edge detector uses a pair of 3x3 convolution masks, one estimating the horizontal gradient and the other estimating vertical gradient. Finally, the segmented objects with different shades of gray color corresponding to each individual object are depicted in Figure 2 (f). Due to the different shapes of the objects within the images, the cell nuclei are identified based on object shape descriptor using the segmented image (Figure 2 (f)), and the unwanted objects such as lymphocytes, stromal cells and neutrophils are removed as shown in Figure 2 (g). The proposed algorithm identified six tumor cell nuclei (Figure 2 (g)) from the original sample image (Figure 2 (a)).

Finally, the cell nuclei are classified into two categories, i.e. stained and unstained. The color components (U and V) are used for the classification, and each pixel is classified as a stained or an unstained pixel. A color threshold is determined using color component pixel values, and all pixels with color component pixel values greater than the threshold are classified into a stained group and all other pixels are classified into an unstained group. Each cell nucleus is classified into stained or unstained according to the fraction of stained pixels. As shown in Figure 2 (h), three cell nuclei are classified as stained and three cell nuclei are classified as unstained.

3. SIMULATION RESULTS

The comparison of the hand counted results by a pathologist and our automated results is listed in Table 1 and Table 2. Typical input image size is 2560x1920, and the proposed technique was evaluated on a test data set consisting of 50 images from 5 different patients. We selected one of 10 images from each patient to train the proposed algorithm (Table 1). It should be noted that once all the parameters are set in the training session, the parameters are fixed while processing all 50 test images (Table 2). In Table 2, the first column (Total) is the average of ten total numbers of cell nuclei of each patient, and the second column (Stained) is the average of ten stained nuclei counts of each patient. The comparison shows no significant difference in total and stained number of tumor cell nuclei. However, after reviewing the output images, it was noted that even though the automated results are identical to the hand counted results, it still misses small number of nuclei and includes small number of false alarms.

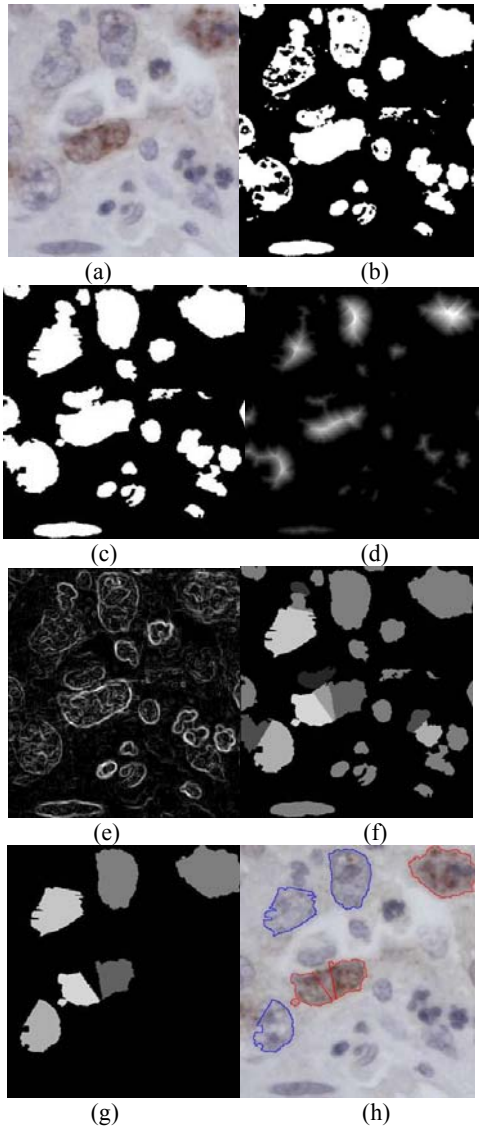

Figure 2: Automated image segmentation example. (a) Original image. (b) Segmented binary image. (c) Segmented image after morphological operations. (d) Distance transform. (e) Edge detected image. (f) Segmented image after watershed transform. (g) Segmented cell nuclei. (h) Classified stained and unstained cell nuclei.

Image	Hand Counted Results			Automated Results		
	Total	Stained	%	Total	Stained	%
image 1	125	26	20.8	129	23	17.8
image 2	283	1	0.4	310	1	0.3
image 3	301	6	2.0	307	5	1.6
image 4	187	3	1.6	168	4	2.4
image 5	450	7	1.6	419	6	1.4

Table 1: Comparison of the hand counted results by a pathologist and automated results using one field of view from each patient.

Patient	Hand Counted Results			Automated Results		
	Total	Stained	%	Total	Stained	%
1	156.9	21.9	14.0	146.9	20.7	14.1
2	263.9	2.8	1.1	301.0	2.4	0.8
3	342.9	4.2	1.2	353.3	3.6	1.0
4	175.6	20.3	11.6	170.0	20.8	12.2
5	414.1	3.9	0.9	399.1	2.6	0.7

Table 2: Comparison of the hand counted results and automated results.

4. CONCLUSION AND FUTURE WORK

In this paper, we have proposed an automated medical image segmentation technique that identifies cell nuclei in medical images for digital pathology, and a quantitative results produced on various test images by the technique have been provided. Our current efforts emphasize the accuracy of stained and unstained cell nuclei counts. The simulation results are encouraging for the further development and evaluation of this method. Future research will be directed to improve the level of accuracy even further over a wide set of different test images and tune the algorithm to handle different diagnosis.

5. REFERENCES

[1] H. Zhou and K. Z. Mao, "Adaptive Successive Erosion-based Cell Image Segmentation for p53 Immunohistochemistry in Bladder Inverted Papilloma," *IEEE Engineering in Medicine and Biology*, pp. 6484-6487, September 2005.

[2] P. Zhao, K. Z. Mao, T. S. Koh, and P. H. Tan, "Automatic Cell Analysis for p53 Immunohistochemistry in Bladder Inverted Papilloma," *IEEE EMBS Asian-Pacific Conference on Biomedical Engineering*, pp. 168-169, October 2003.

[3] K. Z. Mao, P. Zhao, and P. H. Tan, "Supervised Learning-Based Cell Image Segmentation for p53 Immunohistochemistry," *IEEE Transactions on Biomedical Engineering*, vol.53, no.6, pp. 1153-1163, June 2006.

[4] S. Petushi, C. Katsinis, C. Coward, F. Garcia, and A. Tozeren, "Automated Identification of Microstructures on Histology Slides," *IEEE International Symposium on Biomedical Imaging,* vol.1, pp. 424-427, April 2004.

[5] P. Ranefall, L.Egevad, B. Nordin, and E. Bengtsson, "A New Method for Segmentation of Color Images Applied to Immunohistochemically Stained Cell Nuclei," *Analytical Cellular Pathology*, vol.15, pp. 145-156, 1997.

[6] J. G. Postaire, R. D. Zhang, and C. Lecocq-Botte, "Cluster Analysis by Binary Morphology," *IEEE Transactions on PAMI*, vol.15, no.2 pp. 170-180, 1993.

[7] T. Geraud, P. Y. Strub, and J. Darbon, "Color Image Segmentation based on Automatic Morphological Clustering," *IEEE International Conference on Image Processing*, vol.3, pp. 70-73, October. 2001.

[8] P. Ranefall, K. Wester, C. Busch, P-U Malmstrom, and E. Bengtsson, "Automatic Quantification of Microvessels using unsupervised Image Analysis," *Analytical Cellular Pathology*, vol.17, pp. 83-92, 1998.

[9] N. Otsu, "A Threshold Selection Method from Gray-Level Histogram," *IEEE Transactions on Systems Man Cybernetics*, vol.SMC-9, no.1, pp. 62-66, 1979.

[10] S. Beucher and C. Lantuejoul, "Use of Watersheds in Contour Detection," *Proc. International Workshop on Image Processing, Real-Time Edge and Motion Detection/Estimation*, Rennes, September 1979.

[11] R. C. Gonzales and R. E. Woods, *Digital Image Processing*, Addison-Wesley, 1993.

[12] S. H. Landis, T. Murray, S. Bolden and P. A. Wingo, *Cancer Statistics,* CA Cancer J Clin 49, pp. 8-31, 1999.

[13] J. C. Cheville, C. M. Lohse, H. Zincke, A. L. Weaver and M. L. Blute, *Am J Surg Pathol.,* vol.27, no.5, pp. 612-624, 2003.

[14] A. M. Verhagen, E. J. Coulson and D. L. Vaux, "Inhibitor of apoptosis proteins and their relatives : IAPs and other BIRPs," *Genome Biol.*, 2001;2:1-10.

[15] A. S. Parker, F. Kosari, C. M. Lohse, R. Houston Thompson, E. D. Kwon, L. Murphy, D. L. Riehle, M. L. Blute, B. C. Leibovich, G. Vasmatzis and J. C. Cheville, "High expression levels of survivin protein independently predict a poor outcome for patients who undergo surgery for clear cell renal cell carcinoma," *Cancer,* 2006 July 1;107(1):37-45.